Phosphorylation Relieves Autoinhibition of the Kinetochore Motor Cenp-E

Julien Espeut, Amaury Gaussen, Peter Bieling, Violeta Morin, Susana Prieto, Didier Fesquet, Thomas Surrey, Ariane Abrieu

Phosphorylation relieves autoinhibition of the kinetochore motor Cenp-E

Julien Espeut[1,2], Amaury Gaussen[1,2], Peter Bieling[3], Violeta Morin[1,2], Susana Prieto[1,2], Didier Fesquet[1,2], Thomas Surrey[3] and Ariane Abrieu[1,2,4].

[1]Universités Montpellier 2 et 1, IFR122, CRBM.

[2]CNRS, UMR 5237, 1919 Route de Mende, 34293 Montpellier, France.

[3]European Molecular Biology Laboratory, Cell Biology and Biophysics Unit, Meyerhofstrasse 1, 69117 Heidelberg, Germany.

[4]Correspondance should be addressed to A.A. (e-mail: ariane.abrieu@crbm.cnrs.fr).

Running title: **Phosphorylation relieves Cenp-E autoinhibition**

SUMMARY

During mitosis, chromosome alignment depends on the regulated dynamics of microtubules and on motor protein activities. At the kinetochore, the interplay between microtubule-binding proteins, motors and kinases, is poorly understood. Cenp-E is a kinetochore-associated kinesin involved in chromosome congression, but the mechanism by which this is achieved is unclear. Here, we present the first study of the regulation of Cenp-E motility. Using purified full-length (FL) Xenopus Cenp-E protein, we show that FL Cenp-E is a genuine plus-end directed motor. Furthermore, we find that the Cenp-E tail completely blocks the motility of Cenp-E *in vitro*. This is achieved through direct interaction between its motor and tail domains. Finally, we show that Cenp-E autoinhibition is reversed by MPS1 or CDK1-Cyclin B mediated phosphorylation of the Cenp-E tail. This suggests a model of dynamic control of Cenp-E motility, and hence chromosome congression, dependent upon phosphorylation at the kinetochore.

INTRODUCTION

The kinetochore-microtubule interface is highly dynamic due to microtubules growing and shrinking. Yet, it is essential to maintain stable kinetochore-microtubule attachments. A large number of proteins that are enriched at the kinetochore have been identified (Musacchio and Salmon, 2007). These include proteins directly binding to the centromere, or to the microtubules, mitotic motors and kinases. Nevertheless, the signals regulating this dynamic architecture remain elusive.

Although the motor Cenp-E, was among the first proteins to be identified at the kinetochore (Yen et al., 1991), its regulation is poorly understood, partly due to the technical challenge of purifying such large protein. Cenp-E is a member of the kinesin-7 subfamily whose

role in chromosome congression has been extensively described in various models (McEwen et al., 2001; Putkey et al., 2002; Schaar et al., 1997; Wood et al., 1997; Yao et al., 2000; Yucel et al., 2000). Cenp-E gene disruption revealed that it is essential for mammalian development, and that it might stabilize kinetochore-microtubule capture (Putkey et al., 2002). Recent evidence from live microscopy experiments suggests that Cenp-E might contribute to chromosome congression by moving unattached kinetochores laterally along kinetochore microtubules towards the spindle equator (Kapoor et al., 2006). This implicates that Cenp-E could be a plus-end directed kinesin *in vivo*. However, the directionality of Cenp-E motility remains controversial. Partially purified Cenp-E was initially described as a minus-end directed kinesin (Thrower et al., 1995), while the recombinant motor domain was shown to move towards the microtubule plus-end *in vitro* (Wood et al., 1997). Furthermore, purified full-length protein was found not to be motile (DeLuca et al., 2001).

To understand how Cenp-E affects the dynamics of the kinetochore-microtubule interface, it is necessary to know its basic kinetic properties and moreover how these properties are regulated. Therefore, we performed *in vitro* microtubule gliding assays with full-length Cenp-E and with Cenp-E fragments. We show that Cenp-E is autoinhibited through direct motor-tail interaction. More importantly, we find that specific phosphorylation of the Cenp-E tail by MPS1 and/or CDK1-Cyclin B, but not by other kinetochore-associated kinases, counteract this autoinhibitory mechanism.

RESULTS

Cenp-E is a plus-end directed dimeric kinesin

We expressed and purified a full-length (FL) 340 kDa Cenp-E construct with a hexahistidine tag at the C-terminus of the protein in baculovirus infected insect cells (Figure 1A). Using gel filtration (Figure 1B) and sucrose gradient centrifugation analysis (Figure 4B), we determined the hydrodynamic properties of purified recombinant Cenp-E at physiological salt concentrations

(Figure 1C), yielding its native molecular weight of 690 kDa. This demonstrates that FL Cenp-E is a dimer. Based on the axial ratio that we could estimate to be 50:1, and on the average diameter of a coiled-coil dimer (2 nm), the size of Cenp-E could be predicted to be 2 nm x 100 nm. Interestingly, its 22 coiled-coil domains (~2000 amino acids) predict a contour length of 280 nm, if Cenp-E is in an extended conformation. This discrepancy suggests that recombinant Cenp-E is not a fully stretched molecule, but probably displays a more compact conformation.

We then performed microtubule-gliding assays in order to assess its function as a microtubule motor. In these assays the movement of microtubules propelled by motors adsorbed to a glass surface is observed by fluorescence microscopy. Using polarity-marked microtubules, we showed that FL Cenp-E moves towards the plus-end of the microtubules with a velocity of 14.1 ± 3.6 nm per second *in vitro* (Figure 1D and 4D, movie 1). This proves that FL Cenp-E is a genuine plus-end directed motor. However, the motility of the full-length protein, although smooth, appears ~7 times slower than the motility of a fragment consisting of the motor domain alone (Wood et al., 1997). We suspected that this decreased velocity could be indicative of autoinhibition of the full-length motor. This autoinhibitory effect could be mediated by the Cenp-E tail domain analogous to what has been shown for kinesin-1 (Coy et al., 1999; Friedman and Vale, 1999). In order to test this hypothesis, we generated three DNA constructs covering different parts of the tail domain of Cenp-E. From the longest construct, which we will refer to as F-tail (full-length tail), we derived 2 shorter fragments, which we call N-tail (N-terminal part of the tail) and C-tail (C-terminal part of the tail) (Figure 1E). Earlier experiments suggested that human Cenp-E tail bears kinetochore and microtubule-binding domains that might not completely overlap (Chan et al., 1998; Liao et al., 1994). Therefore, we first examined the localization of these Cenp-E fragments to kinetochores in Xenopus egg extracts. After depletion of endogenous Cenp-E, the extracts were complemented with Cenp-E tail proteins (Figure S1A). While both F-tail and N-tail localized to the kinetochore, the C-tail protein did not (Figure S1B). However, Cenp-E C-tail did bind to microtubules in cosedimentation assays *in vitro*

(Figure S2A), with a dissociation constant (Kd) of 200 nM (data not shown). Taken together, these results show that a minimal kinetochore (i.e. cargo) binding domain of Cenp-E (N-tail) can be uncoupled from its C-terminal microtubule-binding domain (C-tail).

Cenp-E C-tail inhibits the motility of Cenp-E motor domain via direct interaction

To directly test for an effect of these tail proteins on Cenp-E motility, we constructed a Cenp-E motor domain protein consisting of the first 473 amino-acids of Cenp-E, i.e. the motor domain, the neck and the first coiled-coil domain, tagged with GFP and hexahistidine at its C-terminus. Using *in vitro* gliding assays, we measured an average velocity of 93.5 ± 7.2 nm per second for the Cenp-E motor (Figure 2A & 3C, movie 2), consistent with what had been previously measured for a non-GFP tagged Cenp-E motor construct (Wood et al., 1997). Because the Cenp-E tail directly binds to microtubules, we slightly modified the classical protocol for gliding assays in the presence of Cenp-E tail. Glass slides were saturated with 20 μg BSA per flow cell after adsorption of the Cenp-E motor, but before addition of the tail. We checked that after BSA saturation followed by Cenp-E C-tail addition, microtubules could not directly bind to the surface in the absence of the motor. The addition of Cenp-E N-tail had no effect on the gliding of Cenp-E motor (data not shown), while both F-tail and C-tail slowed down the velocity of Cenp-E motor to a similar extent. Because the F-tail protein had a tendency to aggregate, we concentrated our efforts on the effect of Cenp-E C-tail. Addition of increasing doses of Cenp-E C-tail gradually reduced the microtubule gliding velocity (data not shown), and addition of Cenp-E C-tail at the same concentration as the motor in solution, completely inhibited microtubule movement (Figure 2A, movie 3).

In order to further understand how Cenp-E C-tail could directly inhibit Cenp-E motor, we measured Cenp-E motor ATPase rates in the presence of increasing concentrations of Cenp-E C-tail. In solution, the maximal microtubule stimulated ATPase rate, k_{cat}, for Cenp-E motor was 14 ± 1 s^{-1} (the number of ATP hydrolysed per second per molecule) (Figure 2B). If Cenp-E uses

a processive walking action, like kinesin-1, then it would take 8 nm steps and hydrolyses 1 ATP molecule per step. Our measured maximal mechanical velocity (106 nm per second) and the maximal ATPase rate (14.1 s^{-1}) are consistent with this behavior. Again, we found that addition of increasing concentrations of Cenp-E C-tail gradually inhibited motor activity. Total inhibition of Cenp-E motor ATPase was achieved at a concentration of 1.6 μM of Cenp-E C-tail (Figure 2B). Even though Cenp-E C-tail bound to microtubules in cosedimentation assays, inhibition of motor activity was most likely not caused by sterically blocking motor stepping along microtubules as a consequence of crowding the microtubule with tail molecules: half maximal inhibition of the ATPase rate was obtained at a tail concentration that is 40-fold lower than the saturating tubulin concentration present in these assays.

Therefore, we tested by surface plasmon resonance analysis if Cenp-E motor and C-tail directly interact and we found that this was, indeed, the case (Figure 2C). The measured dissociation constant of about 3 μM does however, not necessarily reflect the strength of the interaction between the motor and tail domains in the native protein, where they are part of the same molecule. The intramolecular interaction between Cenp-E motor and tail in the full-length molecule is expected to be much stronger than the intermolecular interaction between independent motor and tail fragments. Altogether, these results demonstrate that a direct motor-tail interaction inhibits Cenp-E motility.

C-tail dependent inhibition of Cenp-E is reversed by phosphorylation

How could the Cenp-E motor domain be liberated from the inhibitory interaction with its tail domain? Phosphorylation of human Cenp-E tail by CDK1-Cyclin B (Liao et al., 1994), and MAPK (Zecevic et al., 1998) has been reported previously. Furthermore, a recent mass spectrometry study of the spindle phosphoproteome identified at least eight phosphorylated amino acids on Cenp-E *in vivo* (Nousiainen et al., 2006), among which three are in the C-tail domain of Cenp-E. While two of these sites match the CDK1 and/or MAPK consensus

phosphorylation sequence, the third one does not, suggesting that additional kinase(s) phosphorylate Cenp-E *in vivo*. In order to assess whether Cenp-E C-tail inhibition of the motor domain could be regulated by phosphorylation, we probed for phosphorylation of Cenp-E by MPS1, a kinetochore-localized kinase (Abrieu et al., 2001), and CDK1-Cyclin B *in vitro*. Indeed, Cenp-E C-tail is heavily phosphorylated *in vitro* by both kinases (Figure 3A). Cenp-E N-tail is not phosphorylated *in vitro* by either kinase (data not shown). Strikingly, phosphorylation of Cenp-E C-tail by WT MPS1 or CDK1-Cyclin B completely reverses its inhibitory effect towards Cenp-E motor ATPase in solution (Figure 3B). This reversal of the inhibitory effect of the Cenp-E tail is a consequence of the MPS1 kinase activity because a kinase-dead version of MPS1 does not prevent Cenp-E C-tail from inhibiting Cenp-E motor ATPase activity (Figure 3B). Furthermore, the presence of MPS1 does not affect the ATPase activity of the motor in the absence of the tail excluding that MPS1 has a direct activating effect on the motor itself (Figure 3B).

Similar results were obtained in gliding assays. Cenp-E C-tail phosphorylated by either WT MPS1 or CDK1-Cyclin B was unable to inhibit the gliding of Cenp-E motor. As expected, in the presence of kinase-dead MPS1, the C-tail domain still fully inhibits Cenp-E motor gliding (Figure 3C). Furthermore, we can exclude an indirect effect of CDK1-Cyclin B towards the motor or the microtubules, because inhibition of CDK1-Cyclin B by roscovitine after phosphorylation of the tail but before addition of the phosphorylated tail to the assay, did not affect Cenp-E motor velocity (data not shown). Furthermore Cenp-E C-tail phosphorylation by other kinetochore-associated kinases such as MAPK or PLK1 (Musacchio and Salmon, 2007), did not significantly relieve the tail-mediated autoinhibition of Cenp-E motor gliding (data not shown). Phosphorylation of Cenp-E C-tail by MPS1 or CDK1-Cyclin B does not prevent Cenp-E C-tail from associating with microtubules (Figure S2B). Again, this observation suggests that the inhibitory effect of the Cenp-E tail is not a consequence of simply blocking the track for Cenp-E movement sterically, through binding of the tail domain to microtubules. Addition of WT MPS1 or CDK1-Cyclin B alone to Cenp-E motor did not alter its microtubule gliding behaviour (data not

shown). Altogether, these results demonstrate that the phosphorylation of Cenp-E C-tail by CDK1-Cyclin B or MPS1 prevents the tail domain of Cenp-E from inhibiting the plus-end directed gliding of the Cenp-E motor domain.

Next, we asked whether the full-length Cenp-E could be regulated by MPS1 or CDK1 phosphorylation. Since we used recombinant protein purified from asynchronously growing eukaryotic cells, it is likely that the major fraction of the Cenp-E molecules are non-phosphorylated by mitotic kinases. We therefore phosphorylated FL Cenp-E by CDK1-Cyclin B or MPS1 *in vitro* (Figure 4A), and then evaluated its hydrodynamic properties by sucrose gradient centrifugation analysis (Figure 4B). FL Cenp-E phosphorylated by MPS1 or CDK1 sedimented with a lower sedimentation coefficient (7.7 S) than unphosphorylated FL Cenp-E (9.2 S). This indicates that phosphorylation of FL Cenp-E affects its overall shape. Furthermore, phosphorylation of the FL Cenp-E by either kinase stimulated the ATPase activity of FL Cenp-E (Figure 4C). Finally, phosphorylation of FL Cenp-E significantly increases its average speed to levels close to the motor domain alone (Figure 4D), since FL Cenp-E phosphorylated by MPS1 or CDK1-Cyclin B supports microtubule gliding with an average velocity of 62.5 ± 17.1 and 61.0 ± 18.6 nm per second, respectively.

DISCUSSION

Taken together, our results show that Cenp-E plus-end directed motility is inhibited by direct motor-tail binding, which is reversed by MPS1 and/or CDK1-Cyclin B dependent phosphorylation of its C-tail domain. Cenp-E N-tail domain is responsible for anchoring Cenp-E at the kinetochore, and this cargo-binding step, could be part of the mechanism relieving Cenp-E autoinhibition *in vivo*. Phosphorylation of Cenp-E C-tail promotes some structural change, which possibly ‘unlocks’ Cenp-E to drive the movement of the kinetochore towards the metaphase plate. Because MPS1 is highly concentrated at the kinetochore (Abrieu et al., 2001),

while CDK1-Cyclin B is abundant throughout the cell in mitosis, it is plausible that MPS1 is the dominant kinase that activates Cenp-E at the kinetochore. In accordance with this model, MPS1 depletion promotes congression defects in HeLa cells (Fisk et al., 2003). Together with our data, this suggests that MPS1 could regulate chromosome congression through direct control of Cenp-E motility. Exhaustive mapping of Cenp-E phosphorylation sites will be required to carefully dissect the contribution of the two kinases *in vivo*.

Remarkably, MPS1 or CDK1-Cyclin B dependent phosphorylation does not affect Cenp-E C-tail binding to microtubules. This result seems to contradict earlier experiments reporting that when unphosphorylated, a fragment of human Cenp-E tail (the last 368 aa) does bind to microtubules *in vitro*, while the fragment phosphorylated by CDK1-Cyclin B does not (Liao et al., 1994). We do not think that this discrepancy can be explained by the difference in the fragment sizes since we determined that all CDK1 phosphorylation sites are in the C-tail, and not in the N-tail domain. This conflicting result might reflect species specificities or differences between the protocols of the pull-down assays. Our finding that phosphorylated Cenp-E C-tail still binds to microtubules opens the possibility that it could contribute to stabilize microtubule-kinetochore interactions, in addition to regulating the activity of the motor domain. Because we are showing that the second, ATP-independent, microtubule-binding domain of Cenp-E is not down-regulated by phosphorylation, this could provide a mean for Cenp-E to bundle adjacent microtubules at the kinetochore in prometaphase. This unexpected observation provides new mechanical insight into earlier data showing that in mammalian cells, perturbation of Cenp-E by inhibition or gene excision reduces microtubule number at the kinetochore (McEwen et al., 2001; Putkey et al., 2002). However, we also found that when the motor domain of Cenp-E is prevented from binding to microtubules (in the presence of ADP), FL Cenp-E does not bind to microtubules *in vitro* (Figure S3). This result, which is in accordance with what was demonstrated for kinesin-1 (Hackney and Stock, 2000), challenges the view that this cryptic microtubule-binding site could bind to microtubules *in vivo*.

The mechanism of Cenp-E autoinhibition appears to be tail-mediated and therefore similar to the one described for kinesin-1 (Coy et al., 1999; Friedman and Vale, 1999). Although FL Cenp-E does not bind to microtubules in the presence of ADP, it does efficiently bind to microtubules in the presence of AMP-PNP (Figure S3). This means that autoinhibited FL Cenp-E can still bind to microtubules via its motor domain. Therefore, the most likely mechanism of inhibition by the C-tail domain is that it blocks the biochemical cycle of the motor, as proposed for kinesin-1 (Coy et al., 1999; Hackney and Stock, 2000). However, this mechanism of inhibition is distinct from kinesin-1 in several ways. First, in the case of Cenp-E, there is no report of associated light chains that could contribute to its autoinhibition. Second, as we could uncouple the kinetochore-binding domain (N-tail), from the motor inhibiting domain (C-tail), we could show that for Cenp-E, it is not the cargo-binding part of the tail, which is inhibiting the motor. Third, for kinesin-1, autoinhibition appears to be mediated by the 'IAK' motif (Hackney and Stock, 2000; Seiler et al., 2000; Cai et al., 2007), a sequence that is absent from Xenopus Cenp-E tail. Structural work will be required to carefully map the motor-tail interacting domains of Cenp-E. Altogether, this provides a distinct regulatory mechanism, which could favour the rational design of specific Cenp-E inhibitors.

EXPERIMENTAL PROCEDURES

Protein purification and antibody production

Xenopus FL Cenp-E was subcloned into a modified pFastBac 1 plasmid engineered to harbor a 6His tag at the C-ter of FL Cenp-E, and was purified as described (Abrieu et al., 2000). Cenp-E motor was obtained by subcloning amino acids 1-473 of Cenp-E into a modified pET 21a vector encoding a C-ter GFP (Clontech) upstream of a C-ter 6His tag. Cenp-E C-tail (aa 2717-2954), Cenp-E N-tail (aa 2338-2695), and Cenp-E F-tail (aa 2398-2954) were subcloned into a pRSET vector (Invitrogen). These constructs were transformed into *E. coli* Rosetta (DE3) pLys S, and proteins were purified using Ni-NTA beads (Amersham). The proteins were eluted in the

presence of 250 mM imidazole, and subsequently dialyzed into 50 mM MOPS pH 7, 250 mM KCl, 0.5 mM EGTA, 2 mM $MgCl_2$, 10 % glycerol. For antibody production, a larger Cenp-E tail (L-tail) construct (aa 2277-2954) was introduced into a pET102/D-TOPO vector, expressed and purified according to the manufacturer's instructions for insoluble proteins (Invitrogen). This protein was used to immunize a rabbit. The serum was affinity-purified on immobilized Cenp-E L-tail protein. GST-MPS1 WT and kinase-dead constructs were expressed and purified as described (Abrieu et al., 2001). CDK1-Cyclin B was purchased from New England Biolabs.

Hydrodynamic analysis of recombinant FL Cenp-E

The sedimentation coefficient of FL Cenp-E was determined by sucrose density centrifugation (5-30%). Protein standards and their sedimentation coefficient (in S) were: bovine serum albumin (4.73 S), beta amylase (8.9 S), apoferritin (18 S) and thyroglobulin (19.4 S) (SIGMA). The Stokes radius was measured by gel filtration analysis on a Superose 6 column (Pharmacia). FL Cenp-E was detected by Western blot using the purified anti-Cenp-E tail antibody. Protein standards and their Stokes radii (in nm) were: bovine serum albumin (3.55), beta amylase (5.4), apoferritin (6.1) and thyroglobulin (8.5). The sedimentation coefficients and Stokes radii were calculated as described (Klose and Bird, 2004) and were then used to calculate the native molecular weight and friction coefficient for FL Cenp-E (Siegel and Monty, 1965). Assuming that Cenp-E is a prolate ellipsoid, we could extrapolate its axial ratio from its native molecular mass and friction coefficient (Squire et al., 1968).

ATPase and motility assays.

Steady-state ATPase activity at 25 ± 1°C was measured in ATPase assay buffer (10 mM imidazole pH 6.8, 5 mM K-acetate, 4 mM Mg-acetate, 2 mM EGTA, 0.1 mg/ml bovine serum albumine) containing 10 mM Mg-ATP, 4 μM paclitaxel, and 20 μM of paclitaxel-stabilized microtubules using the MESG-PNP assay (Molecular Probes). The Cenp-E motor concentration

was 18 nM. We tested different concentrations of Cenp-E tail between 0 and 1.6 μM. The turnover rates are expressed per number of Cenp-E monomer per second. Sigmoidal dose-response curve fitting was realized using the Graph Pad Prism software. Average speeds were determined in motility assays by measuring gliding of paclitaxel-stabilized, rhodamine-labeled microtubules over a motor coated glass surface during 3 minutes (Bringmann et al., 2004). For FL Cenp-E motility assays, the glass slides were precoated with anti-6His monoclonal antibody (Serotec). To determine the directionality of FL Cenp-E we used polarity-marked, paclitaxel-stabilized microtubules (Bringmann et al., 2004). Microtubule movements were observed by fluorescence microscopy (Leica DM 4500 B & objective 63x; CoolSnap HQ camera from Roper Scientific, Metamorph software).

Kinase assays

Cenp-E C-tail (1.6 μM) or FL Cenp-E (0.3 μM) were incubated for 60 minutes at room temperature in the presence of 35 nM of MPS1 (WT or KD), or 15 nM of CDK1-Cyclin B, in the presence of 100 μM ATP. When required, 0.1 μCi/μl of γ-^{32}P-ATP was added to the reaction.

Surface plasmon resonance analysis (Biacore).

Cenp-E motor/tail binding interactions were characterized by Surface Plasmon Resonance using the Biacore 2000 system (BIAcore AB). Experiments were carried out at 25°C, under a constant flow rate of 20 μl/min, using buffer filtered and degassed before use (50 mM MOPS pH 7, 150 mM KCl, 0.5 mM EGTA, 2 mM $MgCl_2$). Cenp-E motor was immobilized on a channel of a CM5 sensor chip using an amine coupling kit at a concentration of 5.5 μM for 2 minutes. After immobilization, the Cenp-E motor and control channels were blocked by a 5-minute injection of 1 M ethanolamine at pH 8.5. Following blocking, different concentrations (0.8 μM to 3.2 μM) of Cenp-E C-tail diluted in running buffer were passed over the surfaces followed by 200 seconds

dissociation. The regeneration of the surface was performed with 10 mM glycine pH 2. The net Response Unit (RU) was obtained by subtracting the baseline from the sample response.

ACKNOWLEDGEMENTS

We are indebted to M.C. Guérin and J. Martin for their expertise with the Biacore 2000, to O. Coux and M. Morris for their expertise with FPLC, to Montpellier RIO Imaging facility of Campus CNRS, route de Mende, and to the platforms of the IFR122. We thank D. Fisher and J. Ewbank for reading the manuscript. This work was supported by grants to AA from the European Community ('Spindle Dynamics' and 'MitoCheck'), the Concern Foundation (USA), the French Research Ministry (ACI 'jeunes chercheurs') and grants from the French anti-Cancer Research Association ('ARC' 4600 & 3147). Salary for AA is provided by INSERM (French Medical Health and Research Institute). JE and AG received PhD fellowships from the French research ministry, and subsequently from ARC (Association pour la Recherche contre le Cancer) and FRM (Fondation pour la Recherche Médicale) respectively. The authors declare that they have no competing financial interests.

REFERENCES

Abrieu, A., Kahana, J.A., Wood, K.W., and Cleveland, D.W. (2000). CENP-E as an essential component of the mitotic checkpoint in vitro. Cell *102*, 817-826.

Abrieu, A., Magnaghi-Jaulin, L., Kahana, J.A., Peter, M., Castro, A., Vigneron, S., Lorca, T., Cleveland, D.W., and Labbe, J.C. (2001). Mps1 is a kinetochore-associated kinase essential for the vertebrate mitotic checkpoint. Cell *106*, 83-93.

Bringmann, H., Skiniotis, G., Spilker, A., Kandels-Lewis, S., Vernos, I., and Surrey, T. (2004). A kinesin-like motor inhibits microtubule dynamic instability. Science *303*, 1519-1522.

Cai, D., Hoppe, A.D., Swanson, J.A., and Verhey, K.J. (2007). Kinesin-1 structural organization and conformational changes revealed by FRET stoichiometry in live cells. J Cell Biol *176*, 51-63.

Chan, G.K., Schaar, B.T., and Yen, T.J. (1998). Characterization of the kinetochore binding domain of CENP-E reveals interactions with the kinetochore proteins CENP-F and hBUBR1. J Cell Biol *143*, 49-63.

Coy, D.L., Hancock, W.O., Wagenbach, M., and Howard, J. (1999). Kinesin's tail domain is an inhibitory regulator of the motor domain. Nat Cell Biol *1*, 288-292.

DeLuca, J.G., Newton, C.N., Himes, R.H., Jordan, M.A., and Wilson, L. (2001). Purification and characterization of native conventional kinesin, HSET, and CENP-E from mitotic hela cells. J Biol Chem *276*, 28014-28021.

Fisk, H.A., Mattison, C.P., and Winey, M. (2003). Human Mps1 protein kinase is required for centrosome duplication and normal mitotic progression. Proc Natl Acad Sci U S A *100*, 14875-14880.

Friedman, D.S., and Vale, R.D. (1999). Single-molecule analysis of kinesin motility reveals regulation by the cargo-binding tail domain. Nat Cell Biol *1*, 293-297.

Hackney, D.D., and Stock, M.F. (2000). Kinesin's IAK tail domain inhibits initial microtubule-stimulated ADP release. Nat Cell Biol *2*, 257-260.

Kapoor, T.M., Lampson, M.A., Hergert, P., Cameron, L., Cimini, D., Salmon, E.D., McEwen, B.F., and Khodjakov, A. (2006). Chromosomes can congress to the metaphase plate before biorientation. Science *311*, 388-391.

Klose, R.J., and Bird, A.P. (2004). MeCP2 behaves as an elongated monomer that does not stably associate with the Sin3a chromatin remodeling complex. J Biol Chem *279*, 46490-46496.

Liao, H., Li, G., and Yen, T.J. (1994). Mitotic regulation of microtubule cross-linking activity of CENP-E kinetochore protein. Science *265*, 394-398.

McEwen, B.F., Chan, G.K., Zubrowski, B., Savoian, M.S., Sauer, M.T., and Yen, T.J. (2001). CENP-E is essential for reliable bioriented spindle attachment, but chromosome alignment can be achieved via redundant mechanisms in mammalian cells. Mol Biol Cell *12*, 2776-2789.

Musacchio, A., and Salmon, E.D. (2007). The spindle-assembly checkpoint in space and time. Nat Rev Mol Cell Biol *8*, 379-393.

Nousiainen, M., Sillje, H.H., Sauer, G., Nigg, E.A., and Korner, R. (2006). Phosphoproteome analysis of the human mitotic spindle. Proc Natl Acad Sci U S A *103*, 5391-5396.

Putkey, F.R., Cramer, T., Morphew, M.K., Silk, A.D., Johnson, R.S., McIntosh, J.R., and Cleveland, D.W. (2002). Unstable kinetochore-microtubule capture and chromosomal instability following deletion of CENP-E. Dev Cell *3*, 351-365.

Schaar, B.T., Chan, G.K., Maddox, P., Salmon, E.D., and Yen, T.J. (1997). CENP-E function at kinetochores is essential for chromosome alignment. J Cell Biol *139*, 1373-1382.

Seiler, S., Kirchner, J., Horn, C., Kallipolitou, A., Woehlke, G., and Schliwa, M. (2000). Cargo binding and regulatory sites in the tail of fungal conventional kinesin. Nat Cell Biol *2*, 333-338.

Siegel, L.M., and Monty, K.J. (1965). Determination of Molecular Weights and Frictional Ratios of Macromolecules in Impure Systems: Aggregation of Urease. Biochem Biophys Res Commun *19*, 494-499.

Squire, P.G., Moser, P., and O'Konski, C.T. (1968). The hydrodynamic properties of bovine serum albumin monomer and dimer. Biochemistry *7*, 4261-4272.

Thrower, D.A., Jordan, M.A., Schaar, B.T., Yen, T.J., and Wilson, L. (1995). Mitotic HeLa cells contain a CENP-E-associated minus end-directed microtubule motor. Embo J *14*, 918-926.

Wood, K.W., Sakowicz, R., Goldstein, L.S., and Cleveland, D.W. (1997). CENP-E is a plus end-directed kinetochore motor required for metaphase chromosome alignment. Cell *91*, 357-366.

Yao, X., Abrieu, A., Zheng, Y., Sullivan, K.F., and Cleveland, D.W. (2000). CENP-E forms a link between attachment of spindle microtubules to kinetochores and the mitotic checkpoint. Nat Cell Biol *2*, 484-491.

Yen, T.J., Compton, D.A., Wise, D., Zinkowski, R.P., Brinkley, B.R., Earnshaw, W.C., and Cleveland, D.W. (1991). CENP-E, a novel human centromere-associated protein required for progression from metaphase to anaphase. Embo J *10*, 1245-1254.

Yucel, J.K., Marszalek, J.D., McIntosh, J.R., Goldstein, L.S., Cleveland, D.W., and Philp, A.V. (2000). CENP-meta, an essential kinetochore kinesin required for the maintenance of metaphase chromosome alignment in Drosophila. J Cell Biol *150*, 1-11.

Zecevic, M., Catling, A.D., Eblen, S.T., Renzi, L., Hittle, J.C., Yen, T.J., Gorbsky, G.J., and Weber, M.J. (1998). Active MAP kinase in mitosis: localization at kinetochores and association with the motor protein CENP-E. J Cell Biol *142*, 1547-1558.

FIGURE LEGENDS

Figure 1. Dimeric full-length Cenp-E is a plus-end directed motor

(A) Coomassie-stained SDS-PAGE of purified recombinant FL Cenp-E. (B) Gel filtration analysis of FL Cenp-E detected by Western blot. (C) Hydrodynamic properties and dimensions of recombinant FL Cenp-E. (D) Fluorescence microscopy images of a microtubule-gliding assay with surface-immobilized FL Cenp-E and polarity-marked microtubules. The leading brightly labelled minus-end of the moving microtubule indicates plus-end directed motility of FL Cenp-E. Selected frames from one time-lapse series are presented. The arrow points to the initial position of the minus-end of the microtubule. Scalebar, 3 μm. (E) Schematic illustration of the domain structure of Cenp-E showing the two motor domains (yellow circle), separated from the tail domain (blue) by 22 predicted coiled-coil domains (green ovals). The constructs corresponding to the different parts of the protein used in this study are depicted.

Figure 2. Direct interaction between Cenp-E motor and C-tail inhibits Cenp-E motility

(A) Fluorescence images of microtubule gliding assays with surface immobilised Cenp-E motor in the absence (top panel) and in the presence of the same amount of Cenp-E C-tail (bottom panel). Selected frames of gliding microtubules are presented. The arrow and arrowhead point to the initial position of two microtubules. Scalebar, 5 μm. (B) Cenp-E motor ATPase activity in the presence of saturating concentrations of microtubules (20 μM) and ATP (10 mM). Addition of increasing concentrations of Cenp-E C-tail inhibits Cenp-E motor ATPase activity. The concentration required for half-maximal inhibition (apparent Kd) is 480 nM. (C) Surface plasmon resonance analysis (Biacore) of the interaction of soluble Cenp-E C-tail with immobilized Cenp-E motor.

Figure 3. C-tail dependent inhibition of Cenp-E motor is reversed by phosphorylation

(A) *In vitro* phosphorylation of Cenp-E C-tail in the presence of γ-^{32}P-ATP by the following kinases: wild-type (WT) or kinase-dead (KD) MPS1, or CDK1-Cyclin B in presence or absence of roscovitine (20 μM). The protein was stained with Coomassie after SDS-PAGE, and imaged by autoradiography. (B) Cenp-E motor ATPase activity in the presence or absence of Cenp-E C-tail and of KD or WT MPS1, or CDK1-Cyclin B. (C) Velocities in presence or absence of Cenp-E C-tail, and of KD or WT MPS1, or CDK1-Cyclin B are scored by measuring the gliding of individual microtubules (n≥50) in the presence of Cenp-E motor.

Figure 4. Phosphorylation relieves autoinhibition of FL Cenp-E

(A) *In vitro* phosphorylation of FL Cenp-E by MPS1 or CDK1-Cyclin B in the presence of γ-^{32}P-ATP. The protein was stained with Coomassie after SDS-PAGE, and imaged by autoradiography. (B) Sedimentation of FL Cenp-E in the presence or absence of MPS1 or CDK1-Cyclin B is detected by Western blot after sucrose gradient centrifugation. (C) FL Cenp-E ATPase activity in the absence or presence of MPS1 or CDK1-Cyclin B. (D) Velocities of FL Cenp-E in the absence or presence of MPS1 or CDK1-Cyclin B are scored by measuring the gliding of individual microtubules (n≥15). (E) Model for the regulation of Cenp-E motility at the kinetochore. Cenp-E N-tail (N) domain is anchored at the kinetochore (KT). Cenp-E C-tail domain (C) is inhibiting Cenp-E motor domain (yellow ovals) through direct binding. Once Cenp-E C-tail is phosphorylated, FL Cenp-E is subject to a conformational change, allowing its plus-end directed gliding onto microtubules (red line).

Figure 1 Espeut

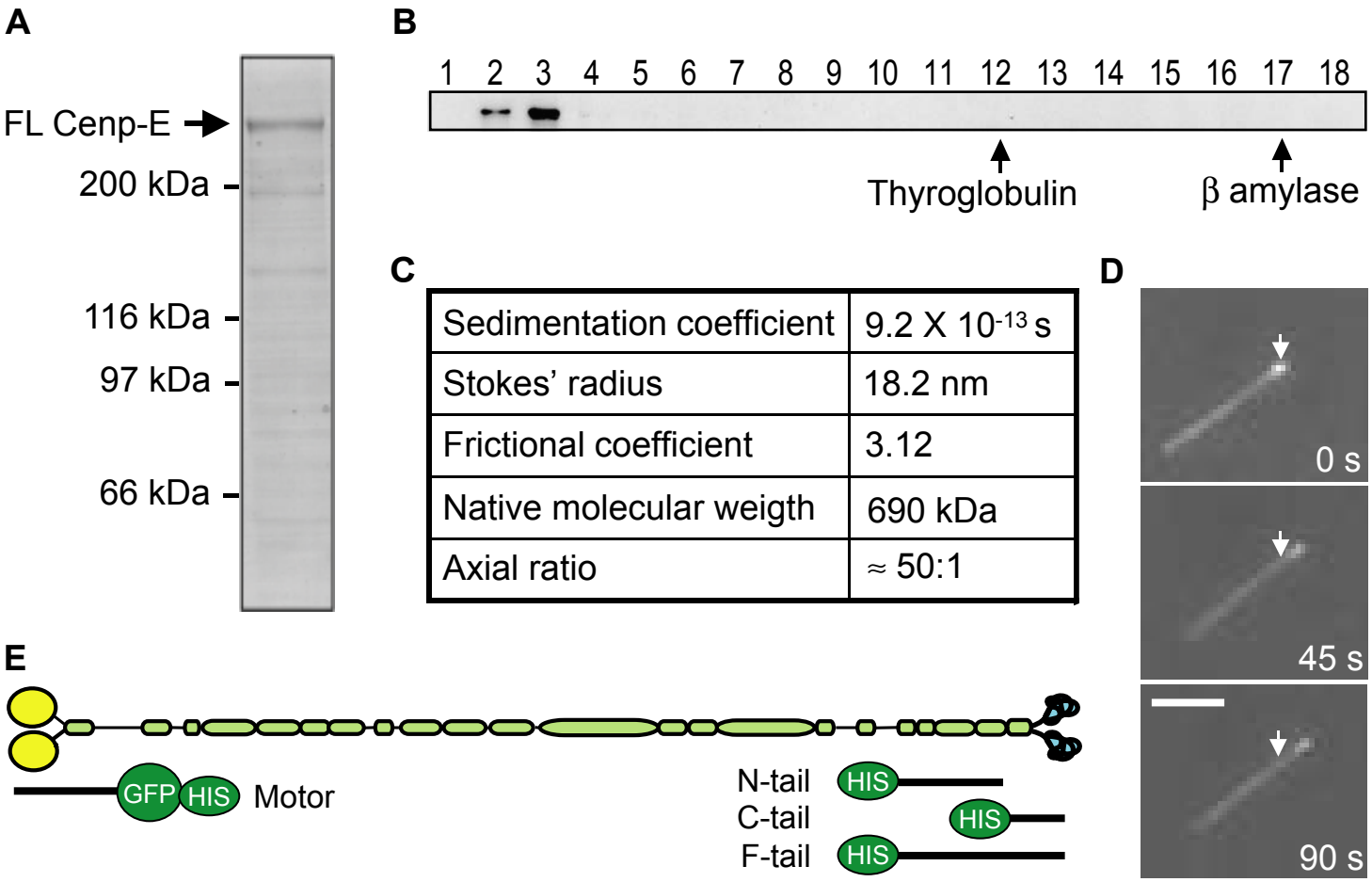

Sedimentation coefficient	9.2 X 10^{-13} s
Stokes' radius	18.2 nm
Frictional coefficient	3.12
Native molecular weigth	690 kDa
Axial ratio	≈ 50:1

Figure 2 Espeut

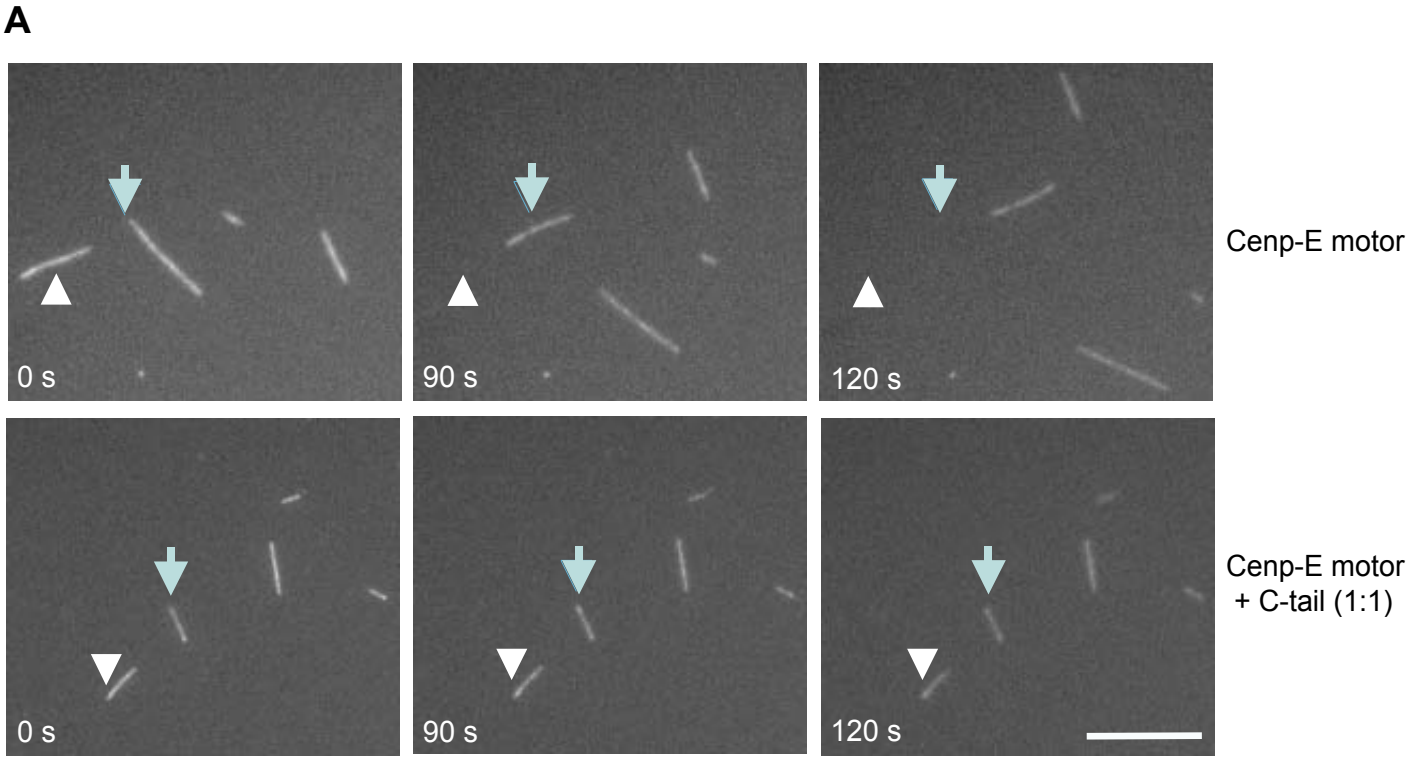

Figure 3 Espeut

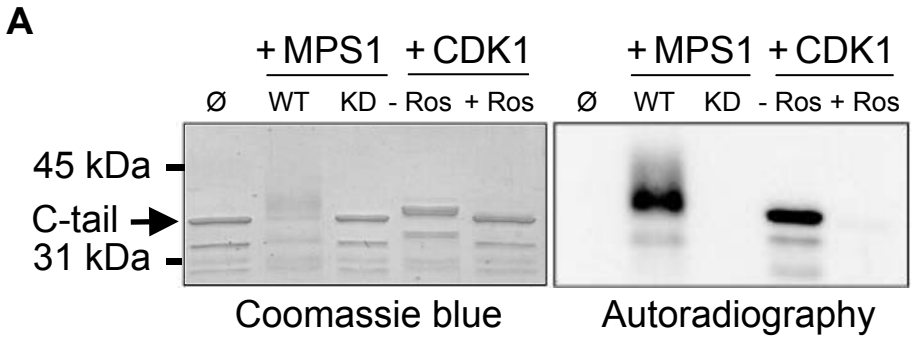

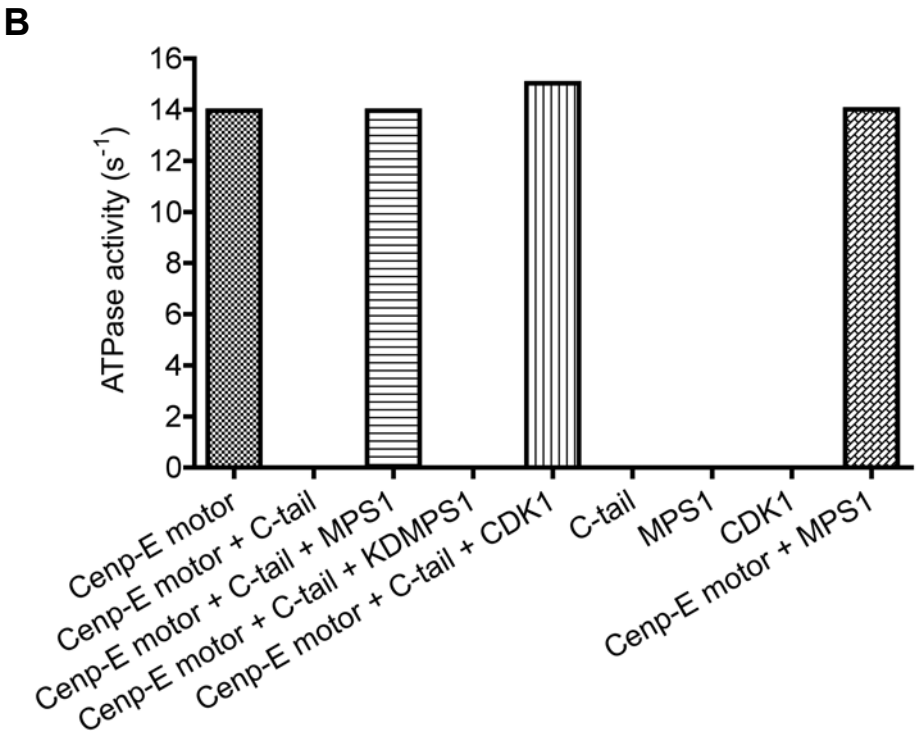

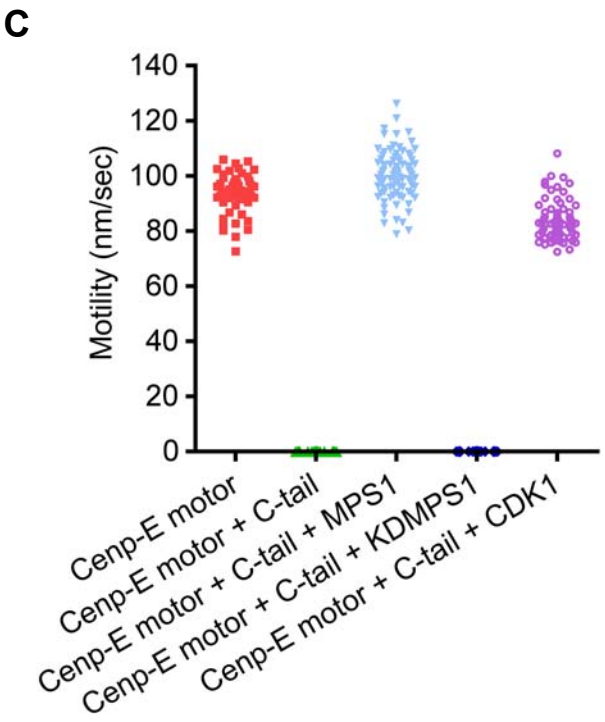

Figure 4 Espeut

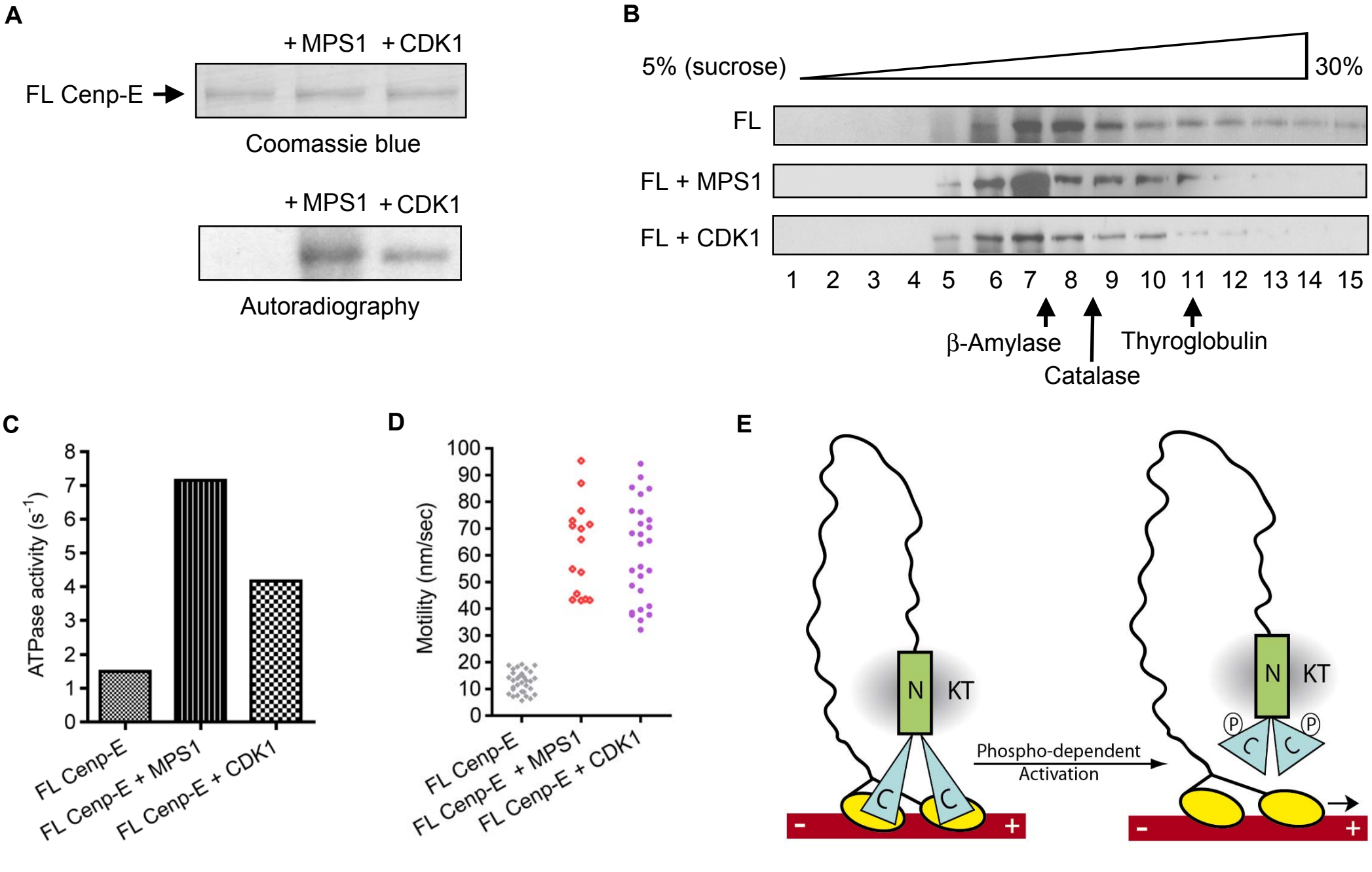

SUPPLEMENTAL DATA

Figure S1. Identification of the kinetochore-binding domain of the Cenp-E tail

(A) Western blot of Xenopus egg extracts (lane 1) or Cenp-E depleted extracts (lanes 2-5) supplemented with Cenp-E F-tail (lane 3), N-tail (lane 4) and C-tail (lane 5). (B) Indirect immunofluorescence staining of Cenp-E at kinetochore (top panels), merged with DAPI staining of DNA (bottom panels). Scalebar, 5 μm.

Figure S2. Cenp-E C-tail interacts with microtubules whether it is phosphorylated or not

(A) SDS-PAGE of Cenp-E C-tail pull-down experiments, in the presence or absence of microtubules (MT), and of the CDK1-Cyclin B kinase buffer supplied by the provider (NEB) are stained with Coomassie. Input (I), supernatant (S) and pellet (P) are loaded. Molecular markers (200; 116, 97; 66; 45; 31 kDa) can be visualized. (B) SDS-PAGE of Cenp-E C-tail and microtubule cosedimentation experiments in the presence of γ-^{32}P-ATP, and in the presence or absence of MPS1 and CDK1-Cyclin B kinase (without CDK1 kinase buffer), stained with Coomassie and imaged by autoradiography.

Figure S3. Cenp-E C-tail does not bind to microtubules when engaged into FL Cenp-E

Phosphorylated or unphosphorylated FL Cenp-E was immobilized onto the glass slides as indicated, in the presence of 10 mM ADP (top panels) or 2 mM AMP-PNP (bottom panels). Binding of paclitaxel-stabilized microtubules onto immobilized FL Cenp-E in the presence of ADP or AMP-PNP is monitored by fluorescence. Scalebar, 15 μm.

Movie 1. FL Cenp-E motility

Movie 2. Cenp-E motor domain motility

Movie 3. Cenp-E motor domain motility in the presence of Cenp-E C-tail

SUPPLEMENTAL METHODS

Immunofluorescence and western blot in Xenopus egg extracts

CSF Xenopus egg extracts were supplemented with demembranated sperm heads in the presence of 10 μg/ml nocodazole for 30 minutes (Abrieu et al., 2000). For immunofluorescence detection, chromosomes were spun through a 40% glycerol cushion in BRB80 buffer (Abrieu et al., 2000). Extracts were depleted from endogenous Cenp-E using anti Cenp-E tail antibody. Recombinant F-tail, N-tail and C-tail proteins were added to roughly endogenous Cenp-E levels. Endogenous Cenp-E and the tail fragments are detected by western blot, or immunofluorescence using the anti-Cenp-E tail antibody.

Microtubule pull down

Phosphorylated and unphosphoryalted Cenp-E C-tail were incubated with a five fold excess of paclitaxel-stabilized microtubules in BRB80, pH 6.8, supplemented with 4 mM DTT in a volume of 30 μl for 15 minutes at room temperature. Microtubules were pelleted at 40,000g for 15 min in a TLA 100 rotor.

Supplemental figure 1 Espeut

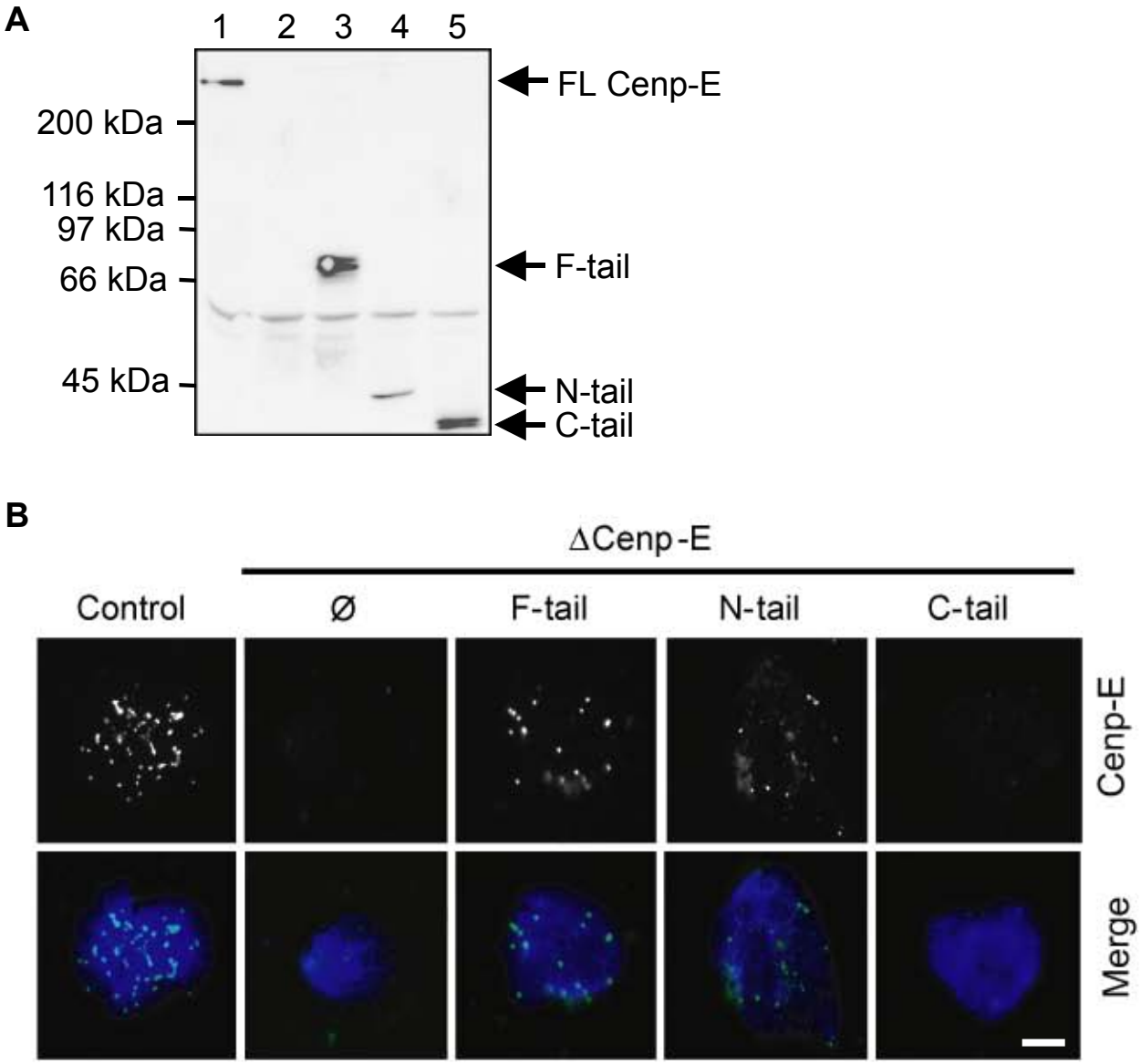

Supplemental figure 2 Espeut

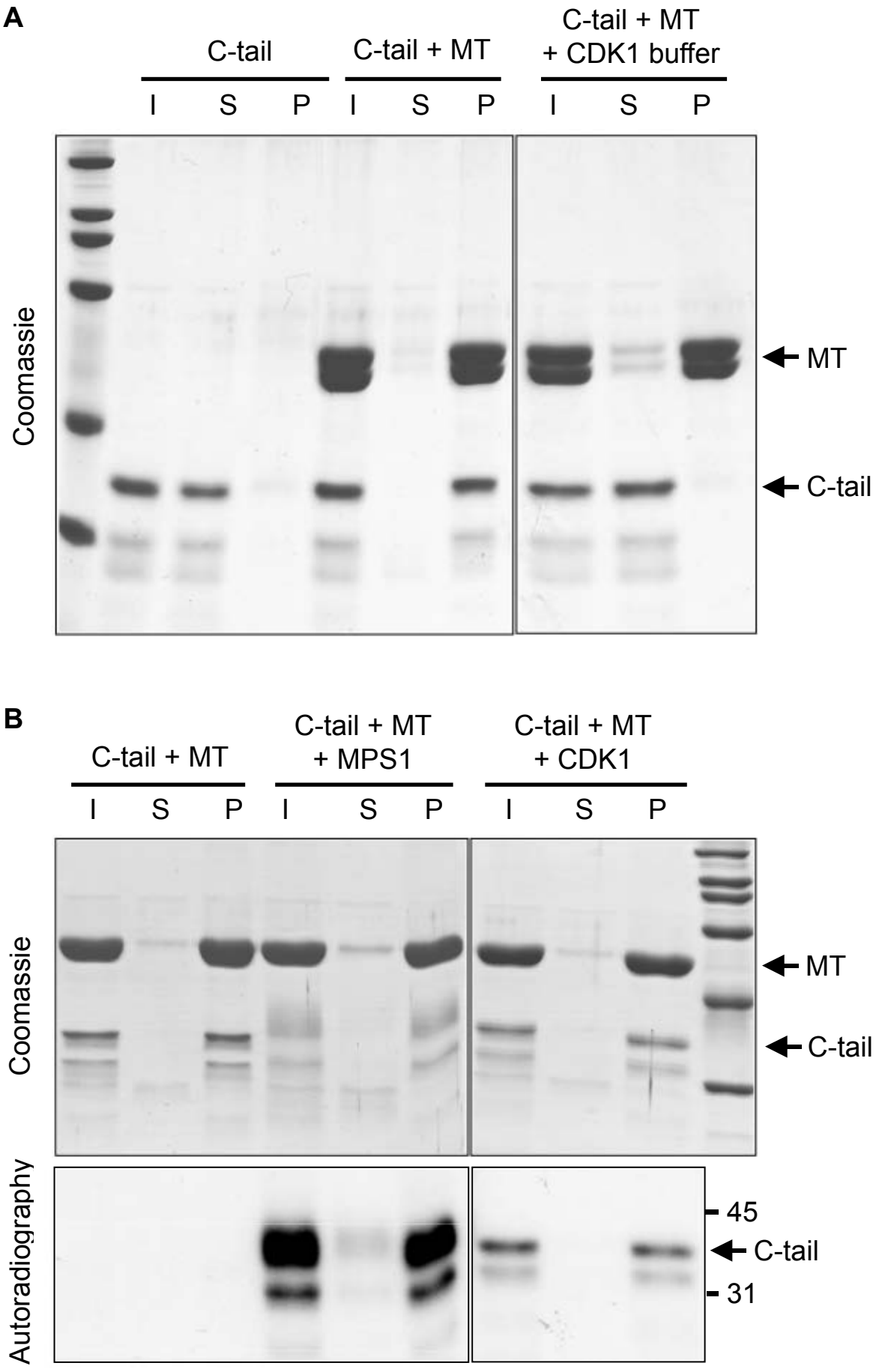

Supplemental figure 3 Espeut